Taiwo, B., Palangio, A., Manuel, J., Monterio, F., Fernandes, N., & Fonseca, D. (2025, January). A mine-to-crusher framework for aggregate operations. Paper presented at the International Society of Explosives Engineers (ISEE)

# A Mine-to-Crusher Framework for Aggregate Operations

**Blessing Taiwo and Andrew Palangio, WipWare Inc.**
**José Manuel and Francisco Monterio, O-Pitblast**
**Nuno Fernandes and Diogo Fonseca, dstgroup quarry**

## Abstract

This research focuses on enhancing the synergy between blasting and primary crushing operations in quarries. A blast operation at dstgroup aggregate quarry in northern Portugal was simulated to fine-tune blasting techniques aimed at optimizing fragmentation indicators. The methodology involves conducting precise blast drill hole surveys, generating detailed terrain 3D models, and integrating these models into blast simulation software to enhance accuracy and optimize production efficiency. The study applies these simulations to test blasts, evaluating improvements in cost-effectiveness, crusher power consumption, and fragmentation efficiency using both aerial and terrestrial image analysis technology. The quarry key performance indicators (KPIs) guide the blast design simulations, ensuring practicality and relevance. The case study blast revealed that implementing optimum blasting techniques can enhance crusher throughput, reduce operational costs, and improve safety. This paper is part one of a three-part technical series where we aim to create a sampling procedure and establish a reliable baseline for the current state of operation. This baseline will be used in subsequent follow-up technical papers to make recommendations and improvements. The outcome of this study provides a framework for quarry operations seeking to enhance their efficiency.

## Introduction

Efficient blasting operations at aggregate quarries depend on a thorough understanding of the rock characteristics (Bahloul et al., 2024). Research shows that the different rock properties on different pit faces have a big effect on how explosive energy is spread, which in turn influences fragmentation, the characteristics of muck piles, and overall productivity (Ma and An, 2008; Dotto, 2024). Although there have been improvements in blasting technology, there is an ongoing requirement for a more comprehensive approach that incorporates accurate geological surveys, advanced modeling, and sophisticated simulation approaches. For aggregate quarries, a major challenge exists due to the lack of a complete framework that integrates blast hole surveys with complex terrain 3D models and their integration into blast simulation software. This gap limits the capacity to optimize blast designs, leading to inefficient energy distribution, poor fragmentation, and reduced production efficiency. One of the most crucial decisions quarry operators should make for productivity assessment is the evaluation of blast results in aggregate stone quarrying.

Mine regulatory authorities also evaluate blast efficiency to ensure environmental safety compliance. When carrying out safe and productive blasting in quarries, there is usually a conflict of interests between the quarry operators and the regulatory authorities. The quarry operators aim to blast and transport the Run-off Mine (ROM) to the processing plant at the lowest possible cost, with minimal or no boulders. However, the regulatory authorities aim to carry out blast operations with minimal environmental disturbance, regardless of the associated costs, fragmentation distributions, and effects on subsequent quarrying processes. This conflict of interest calls for different approaches for evaluating blast efficiency by the various interest groups. Nevertheless, there must be an established framework that considers both process efficiency and environmental safety and is acceptable to all the critical stakeholders in the sector. According to Workman and Eloranta (2003), fragmentation results have both direct and indirect effects on the overall mining operation. The blast material fragment sizes directly impact both material loading and handling operations. Typically, engineers evaluate the particle size distribution by analyzing a representative terrestrial image obtained after a blasting session. Depending on the blast fragment size, inspection frequently assesses and categorizes it as either good or poor. Examining aggregate quarry blasting results holistically can provide insights into the state of controllable and uncontrollable blasting factors. Moreover, the assessment has a significant impact on production efficiency and material crushing capacity, making it a critical factor in aggregate quarries. It is worth noting that an extremely coarse run-off mine reduces the primary crusher's capacity to process material. Insufficient fragmentation will decrease the quantity of smaller particles that can pass through the secondary and tertiary crushing phases, consequently escalating the effort in the subsequent processing stages (Nielsen and Malvik, 1999).

The dstgroup granite quarry operation in Guimarães, Braga, Portugal faces significant challenges in meeting the desired fragmentation needs due to the inconsistent geological features of the quarry formation. These features are particularly concentrated in the northern region, creating variability that impacts the effectiveness of blasting operations. This inconsistency complicates achieving optimal fragmentation for efficient crushing, leading to potential inefficiencies in the quarry-to-crusher process.
This study aims to develop a comprehensive mine-to-crusher framework tailored for the aggregate quarry. As part 1 of a continuous improvement research effort, this paper will establish a baseline by assessing current blasting results and identifying key issues affecting fragmentation. The subsequent parts of the study will implement the recommendations derived from this initial framework to address and resolve the challenges related to achieving crusher-compatible fragmentation, thereby optimizing the overall efficiency of the quarry operations.

## Modelling Framework

Figure 1 describes the mine to crusher framework proposed in this study. At the top of this diagram is the definition of the key input parameters influencing the blast results which include the rock properties, drill hole accuracy, and blast design. The proposed framework involves a holistic approach to improving aggregate quarry crusher efficiency through fragmentation assessment, starting with integration of mine bench topographical data into 3D models, and including point-by-point blast drill hole surveys for blast modeling and simulation.

Rock qualities are well recognized as uncontrollable parameters that have a significant impact on blasting outcomes (Roy et al., 2016). These features can only be accounted for by utilizing detailed information that allows for adjustments to controllable factors. Integration of bench topographical data into 3D models involves using advanced software to create detailed representations of the quarry terrain. The framework's methodology involves using borehole survey data to determine the hole deviation, critical, maximum, and excessive burden distances for every drill hole.

This information is then combined with fragmentation analysis results to assess each blast round. The analysis focuses on identifying oversize fragments and evaluating the crushability of the rock. By integrating these data points, the framework aims to optimize blast designs and improve fragmentation outcomes. This approach ensures more efficient and controlled blasting operations.

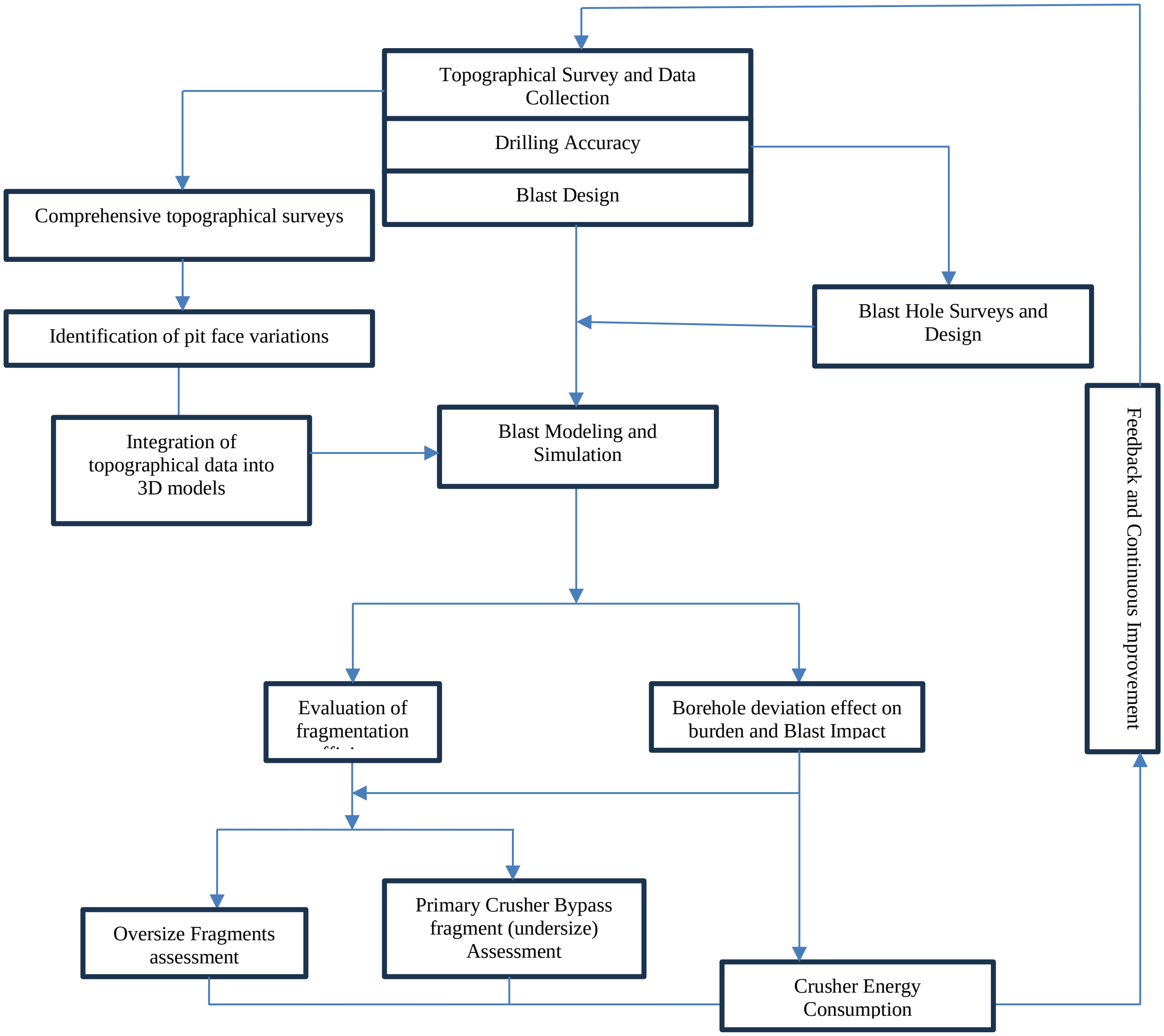

**Figure 1. Mine-to-Crusher Framework Proposed for Aggregate Operations.**

## Methodology

Two blasts (PF 30 and PF 33) were conducted at 11 m bench height, the blast design parameters for PF30 and PF33 are listed in Table 1. Using the study quarry crusher information, hydraulic breaker and the loading operation key performance indicator size, specification curve was design as a control measure, i.e. benchmark to assessing PF30 and PF33 crushability. The PF 30 and PF 33 powder factor and charge design was simulated on O-PitSurface software based on the 3D topographical model (shown in Figure 2). The two blasts were charged using Gemugranel (1.15 g/cm$^3$) Bulk Explosive and Gemulit Super 100_D60 (1.14g/cm$^3$) Cartridge Explosive. The blasts were fired using Shock star 3.6 m_25ms and Shock star 3.6 m_42ms surface connector, Shock star MS_475 in hole delay and TNT Booster T-500. Using DJI FC330 drone, equipped with 4096×3584 resolution camera, Global Position System (GPS) receiver for image georeferencing and with a software that can calculate the main flight parameters while shooting, the 3D model of the case study bench was generated before the drilling operation.

**Table 1. Blast parameter before and after modification.**

| Blast ID | PF 30 | PF 33 |
|---|---|---|
| Bench Height (m) | 11 | 10 |
| Design Burden × Spacing | 3×3 | 3×3 |
| Blast hole Diameter (mm) | 76 | 76 |
| Subdrilling (m) | 0.775 | 0 |
| Average Stemming (m) | 1.9 | 1.8 |
| Average stemming Volume (m$^3$) | 0.011 | 0.008 |
| Total Holes | 66 | 81 |
| Volume (m$^3$) | 6596 | 7348 |
| Specific drilling (m/m$^3$) | 0.117 | 0.11 |
| Maximum Instantaneous Charge (Kg) | 130.9 | 150.7 |
| Powder Factor (Kg/m$^3$) | 0.551 | 0.504 |
| Mean size (mm) | 719.92 | 870.87 |
| $D_{95}$ (mm) | 1508.09 | 1935.83 |
| $D_{80}$ (mm) | 1096.86 | 1394.24 |
| $D_{75}$ (mm) | 1017.70 | 1285.76 |
| $X_{max}$ (mm) | 2770 | 3180 |
| Rosin-Rammler Uniformity Coefficient (n) | 2.5 | 1.61 |

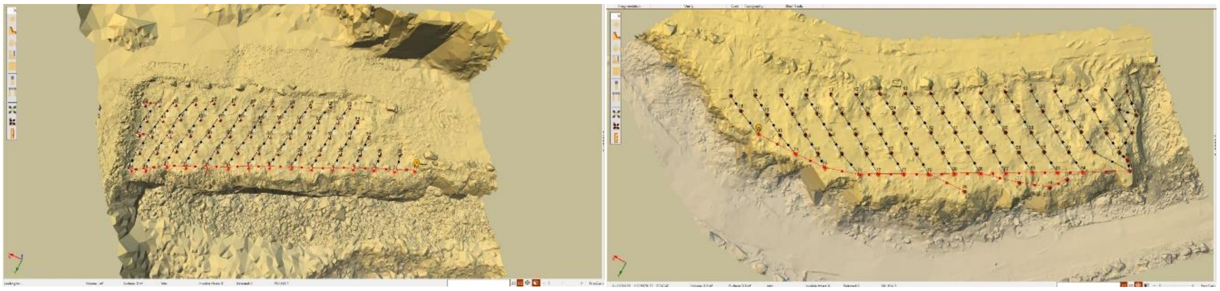

**Figure 2. 3D Topographical model for PF30 and PF 33 blasts.**

As mentioned by Neale (2010), blast drill holes design must be accurate for any blast design to be productive and efficient. Having hole deviations and large tolerances will affect the explosive energy distribution with rock mass during initiation. As part of mine to crusher framework proposed, drilling accuracy assessment was considered to assess and ensure successful implementation of theoretical design onsite. When a drill hole is off target probably because of pegs moving, poor collaring, drill machine or operator defect, and redrilling the effective spacing or burden might be increased in one area and decreased in another, affecting blast induced rock mass damage and crack propagation (Saadatmand Hashemi and Katsabanis, 2020). The trajectory of PF 30 and PF33 production holes was measured and profiled by O-Pitblast engineers using O-Pitdev; the borehole depth profiling was map from the stemming depth downward. The Maximum excessive burden along each drill hole column was calculated using Equation 1.

$$B_{excess} = B_{Max} - B \qquad (1)$$

Where $B_{excess}$ is the maximum excess burden along each drill hole column in m, $B_{Max}$ is the maximum burden as measured along drill hole column in m, and B is the actual design burden in m.

The effect of the drill hole profile on fragmentation and crusher compatibility was assessed to model the blast design variations and evaluate the material crushability.

After each blast round, the fragmentation results were assessed using image analysis technology. For the second blast scenario, different design options were reviewed to find the best adjustments for the case study bench with consideration for the primary crusher inlet size and bypassing size range. After the blasting, drone images were collected using a pre-flight design application (https://www.dronedeploy.com/). To investigate the crushability of the run-off-mine from PF30 and PF33, specification envelope was design for the case study mine crusher gape, oversize material size and crusher outlet using WipFrag 4.0.45 software. The Fragmentation efficiency index was calculated according to Equation 2 (Taji, 2014).

$$FE = 100 - (B + F) \qquad 43 \qquad (2)$$

Where:

B represents percentage of material retained, bigger than crusher gape in %, F is the fine materials percentage which is recommended by Taji (2014) to be approximately one-fifteenth of the boulder's size. As mentioned in the Rafeeian et al. (2019) conference paper, there are multiple ways to assess the degree of fine fragmentation and the presence of oversize fragments in a blast result. This study employed Rafeeian et al.'s (2019) methodology to evaluate oversize materials. The primary crusher's inlet opening dimension was assessed to determine the largest rock suitable to occupy 90% of the feed opening of CJ411 jaw crusher used in dstgroup aggregate quarry. The size of the inlet opening of dstgroup aggregate quarry crusher is 840 mm and the Closed side setting (CSS) range is 120 mm (4.7 in).

## Drill Hole Deviation Results

The survey data from PF30 and PF33 blasts indicate significant variations in toe deviation and burden distances as shown in Table 2. PF33's higher average and maximum bore hole toe deviation suggests greater inconsistency in blast energy distribution compared to PF30. This inconsistency results in uneven fragmentation, potentially increasing the generation of oversized rocks and fines as shown in the fragmentation result despite the simulation of the charge design. The critical burden distance measurement for PF33 was noted to be slightly low which further implies less effective energy distribution in this blast. Figures 3 and 4 show the bore hole design for PF30 and PF33 respectively. The blast plan shows in Figures 3a and 4a with critical toe deviation and burden distance hole marked. The hole survey profile sample for PF30 and PF33 are shown in Figure 3 b&c and 4 b&c respectively. This information was implemented in the framework for each blast charge simulation. The fragmentation analysis results for PF30 and PF33 blasts are discussed in the next section.

**Table 2. Drill hole Deviation Result Statistics for PF30 and PF33 blasts.**

| | Toe Deviation (%) | Critical burden (m) | Maximum Burden (m) |
|---|---|---|---|
| PF 30 | | | |
| Mean | 6.38 | 6.49 | 8.38 |
| Min | 2.2 | 1.26 | 2.16 |
| Max | 15.3 | 13.41 | 14.36 |
| Std | 2.39 | 3.81 | 3.52 |
| PF33 | | | |
| Mean | 9.04 | 5.99 | 8.31 |
| Min | 1.4 | 0.72 | 1.93 |
| Max | 48.2 | 13.53 | 14.73 |
| Std | 5.70 | 3.55 | 3.23 |

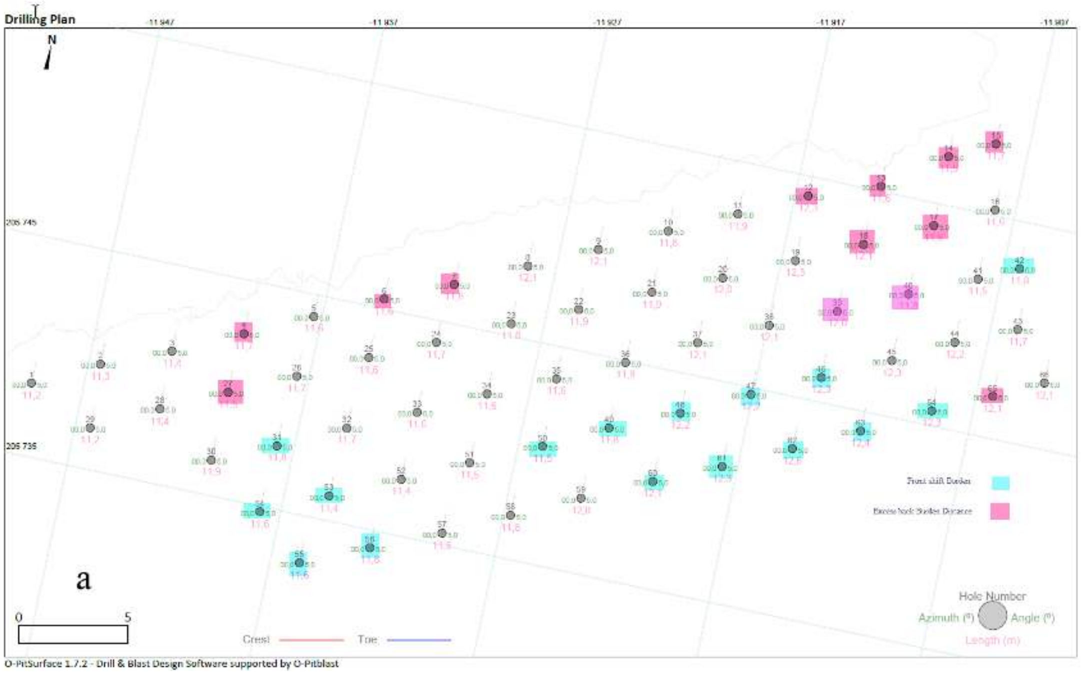

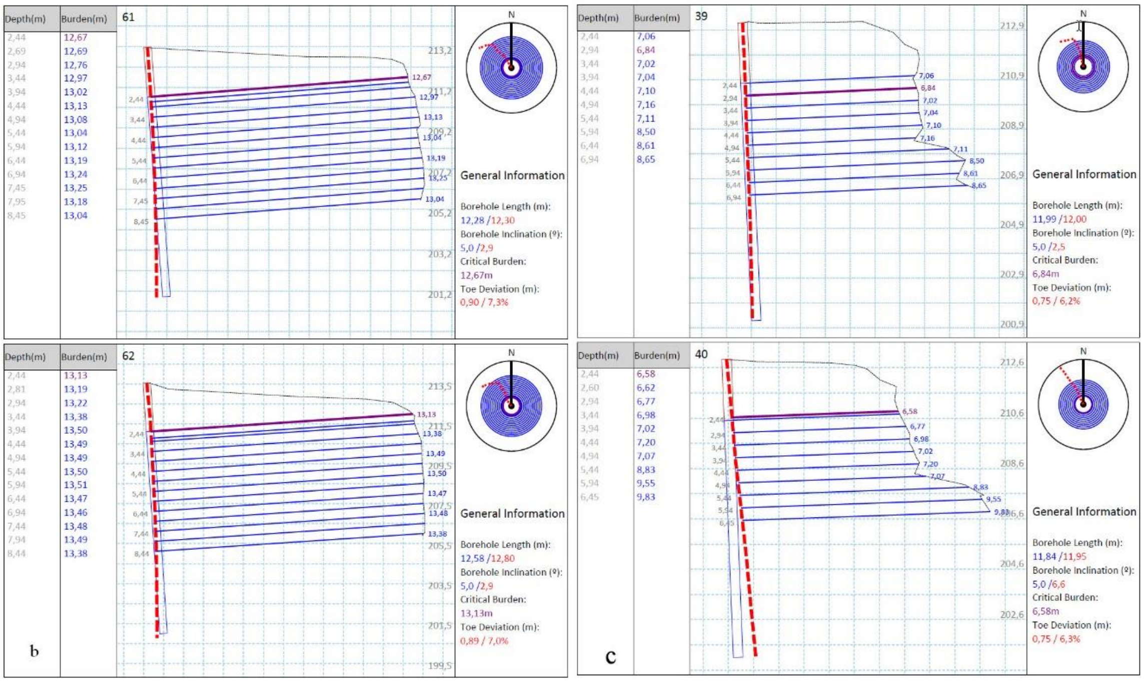

**Figure 3. Blast design plan and hole deviation, (a) PF30 Tie-up plan; (b) Bore hole survey down-hole measurement.**

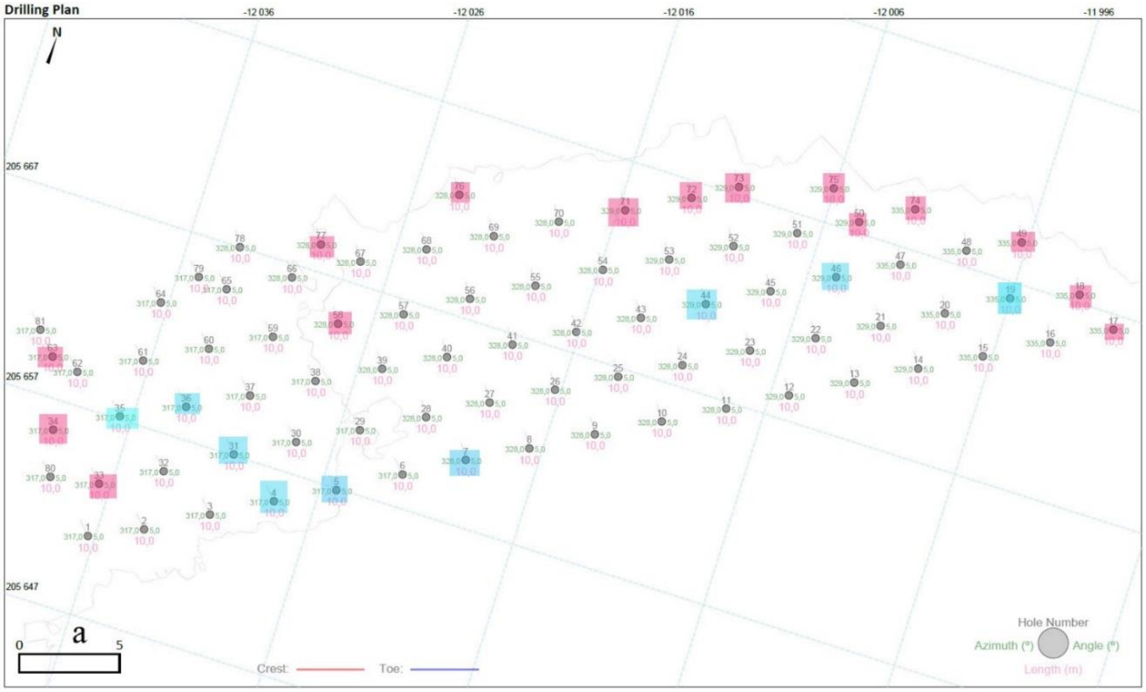

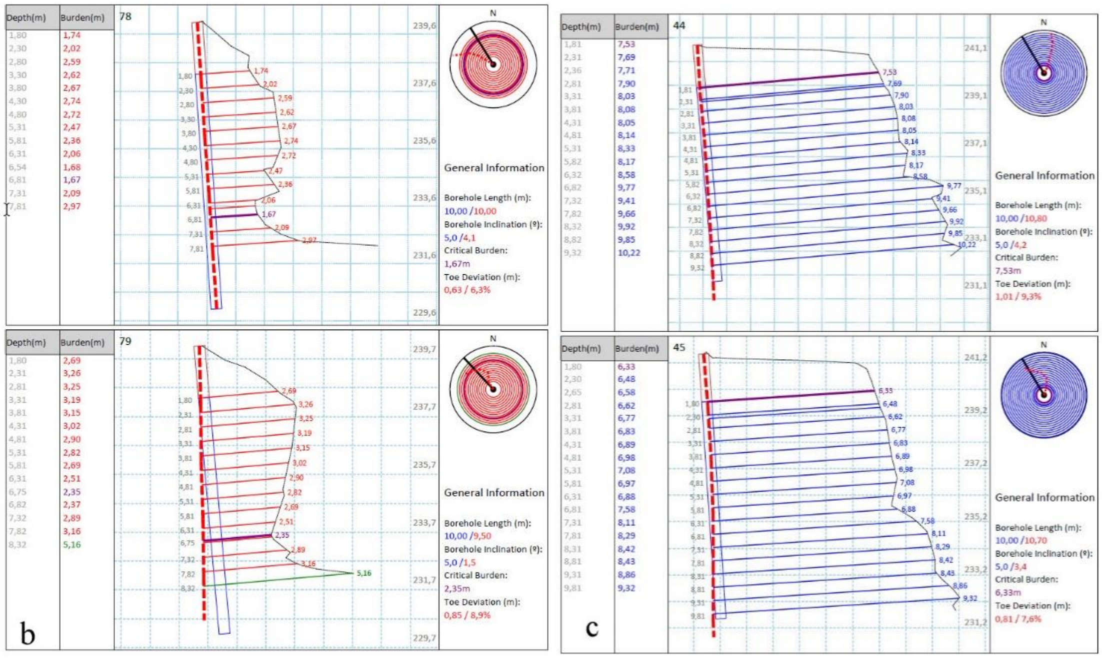

| Depth(m) | Burden(m) |
|---|---|
| 1,80 | 1,74 |
| 2,30 | 2,02 |
| 2,80 | 2,59 |
| 3,30 | 2,62 |
| 3,80 | 2,67 |
| 4,30 | 2,74 |
| 4,80 | 2,72 |
| 5,31 | 2,47 |
| 5,81 | 2,36 |
| 6,31 | 2,06 |
| 6,54 | 1,68 |
| 6,81 | 1,67 |
| 7,31 | 2,09 |
| 7,81 | 2,97 |

General Information

Borehole Length (m):
10,00 /10,00
Borehole Inclination (º):
5,0 /4,1
Critical Burden:
1,67m
Toe Deviation (m):
0,63 / 6,3%

| Depth(m) | Burden(m) |
|---|---|
| 1,80 | 2,69 |
| 2,31 | 3,26 |
| 2,81 | 3,25 |
| 3,31 | 3,19 |
| 3,81 | 3,15 |
| 4,31 | 3,02 |
| 4,81 | 2,90 |
| 5,31 | 2,82 |
| 5,81 | 2,69 |
| 6,31 | 2,51 |
| 6,75 | 2,35 |
| 6,82 | 2,37 |
| 7,32 | 2,89 |
| 7,82 | 3,16 |
| 8,32 | 5,16 |

General Information

Borehole Length (m):
10,00 /9,50
Borehole Inclination (º):
5,0 /1,5
Critical Burden:
2,35m
Toe Deviation (m):
0,85 / 8,9%

| Depth(m) | Burden(m) |
|---|---|
| 1,81 | 7,53 |
| 2,31 | 7,69 |
| 2,36 | 7,71 |
| 2,81 | 7,90 |
| 3,31 | 8,03 |
| 3,81 | 8,08 |
| 4,31 | 8,05 |
| 4,81 | 8,14 |
| 5,31 | 8,33 |
| 5,82 | 8,17 |
| 6,32 | 8,58 |
| 6,82 | 9,77 |
| 7,32 | 9,41 |
| 7,82 | 9,66 |
| 8,32 | 9,92 |
| 8,82 | 9,85 |
| 9,32 | 10,22 |

General Information

Borehole Length (m):
10,00 /10,80
Borehole Inclination (º):
5,0 /4,2
Critical Burden:
7,53m
Toe Deviation (m):
1,01 / 9,3%

| Depth(m) | Burden(m) |
|---|---|
| 1,80 | 6,33 |
| 2,30 | 6,48 |
| 2,65 | 6,58 |
| 2,81 | 6,62 |
| 3,31 | 6,77 |
| 3,81 | 6,83 |
| 4,31 | 6,89 |
| 4,81 | 6,98 |
| 5,31 | 7,08 |
| 5,81 | 6,97 |
| 6,31 | 6,88 |
| 6,81 | 7,58 |
| 7,31 | 8,11 |
| 7,81 | 8,29 |
| 8,31 | 8,42 |
| 8,81 | 8,43 |
| 9,31 | 8,86 |
| 9,81 | 9,32 |

General Information

Borehole Length (m):
10,00 /10,70
Borehole Inclination (º):
5,0 /3,4
Critical Burden:
6,33m
Toe Deviation (m):
0,81 / 7,6%

**Figure 4. Blast design plan and hole deviation, (a) PF33 Tie-up plan; (b) Bore hole survey down-hole measurement.**

## Blast Fragmentation Results

Results from PF30 and PF33 fragmentation analysis are shown in Figure 3. The blast fragmentation assessment reveals big fragments with hot color and fine materials with cool color as shown in Figure 5. The blast fragmentation analysis for PF30 and PF33 presents several critical findings that highlight the challenges encountered during the blasting operation. The borehole survey results further explain the reason behind the poor fragmentation observed. A significant deviation at the toe level in the fourth and last rows of drill holes was detected, suggesting that improper alignment and drilling precision may have contributed to poor fragmentation and insufficient fragmentation at the bench back. PF 30 blast analysis shows big fragment accumulation at the bench front. The borehole deviation result present in Figure 3a reveal information about the reason for the poor fragmentation at this bench flank. For blast PF 33, big fragments are spread along the bench sides as shown in Figure 5b. The mean size, 80 % passing size, maximum size, and blast efficiency for PF33 and PF30 are 870 mm (34 in), 1394.24 mm (55 in), 3180 mm (1235 in) 42.8 % and 720 mm (28 in), 1086.2 mm (43 in), 2777 mm (109 in), 57.52 % and respectively.

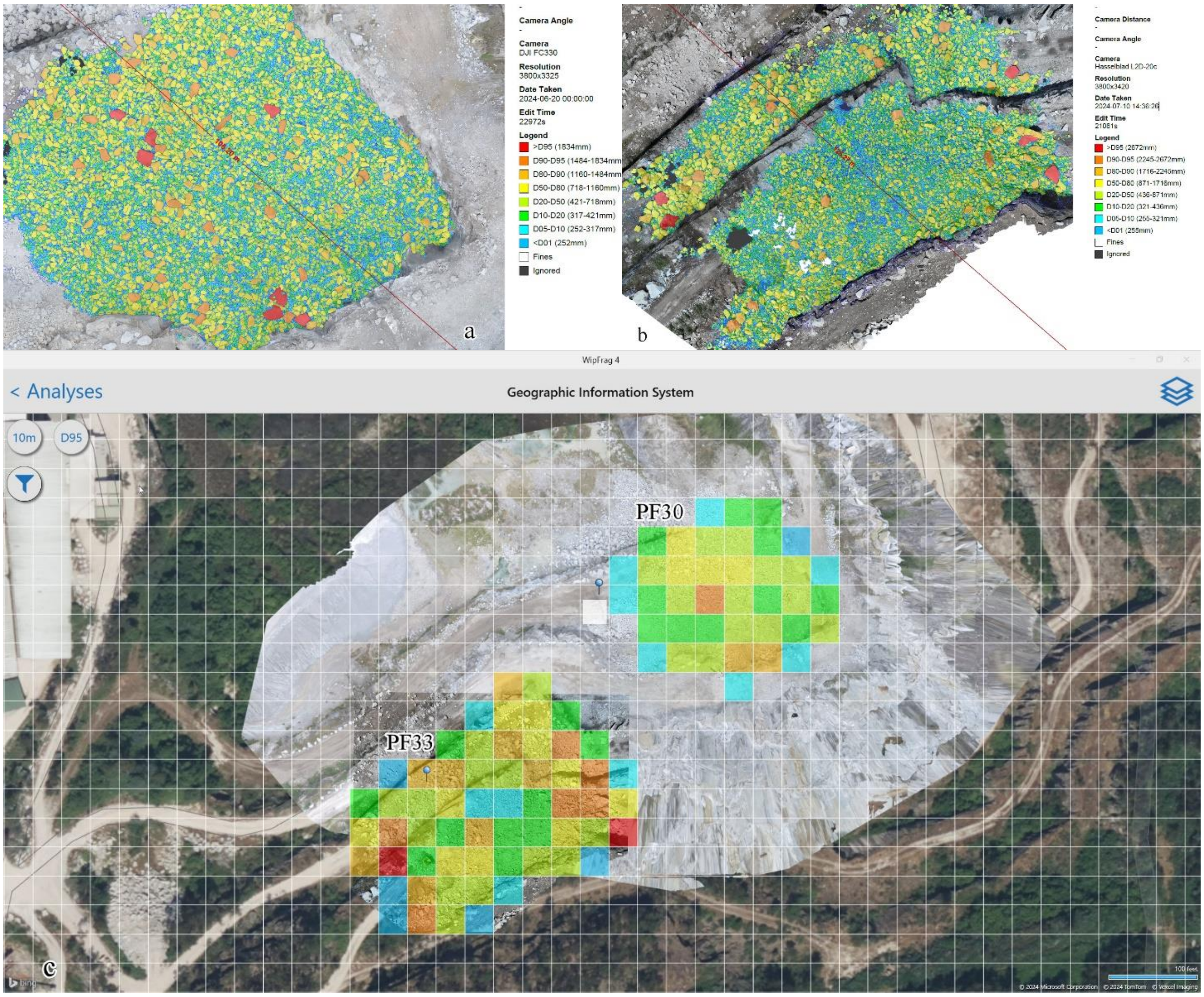

Camera Angle
-
Camera
DJI FC330
Resolution
3800x3325
Date Taken
2024-06-20 00:00:00
Edit Time
22972s

Camera Distance
-
Camera Angle
-
Camera
Hasselblad L2D-20c
Resolution
3800x3420
Date Taken
2024-07-10 14:36:26
Edit Time
21081s

**Figure 5. Fragmentation analysis Result; a. PF30, b. blast, PF33 blast, c. PF30 & PF33 D95 assessment on GIS.**

The blast video analysis identified charge blowouts in PF 33 blast hole 35, 48, 64, 51, 75, and 40, while for PF 30 blast hole 51, 50, 53, 56, and 44. The large number of charge blowouts identified with PF 33 blast is one of the indicating factors responsible for inefficient energy utilization, resulting from excessive burden distance identified from the bore hole survey data. The borehole survey corroborated these findings, pointing to burden irregularities and high toe deviation as the primary causes. These factors and others collectively contribute to the poor fragmentation in both PF 30 and PF 33 by allowing explosive energy to vent prematurely, reducing its effectiveness in breaking the rock.

To evaluate the compatibility of the study blasts with the primary crusher, the framework considered the quarry's crusher feed opening and the Closed Side Setting (CSS). These parameters were used to create a performance assessment area on the particle size distribution (PSD) curve. The quarry utilizes a rock breaker for secondary breakage, and the oversize material was marked in red as the rock breaker region on the PSD, while the crusher-compatible material was indicated in yellow, as shown in Figure 6.

For the crusher compatibility curve, the regions for the crusher-compatible and rock breaker material were kept constant for both blasts PF 30 and PF 33. Each blast's curve comprises three lines: the blue curve represents the actual blast fragmentation without calibration, the red curve shows the calibrated results using the Swebrec method, and the green curve depicts the predicted fragmentation from the simulation software. To account for smaller particles that are too small to be effectively resolved and those hidden behind larger particles, swebrec calibration was used. The results showed that the PF 30 blast was more compatible with the crusher than the PF 33 blast. The simulation predicted oversize material in the upper region of the curve, indicating that the PF 33 blast design was less effective in minimizing oversize material compared to the PF 30 design.

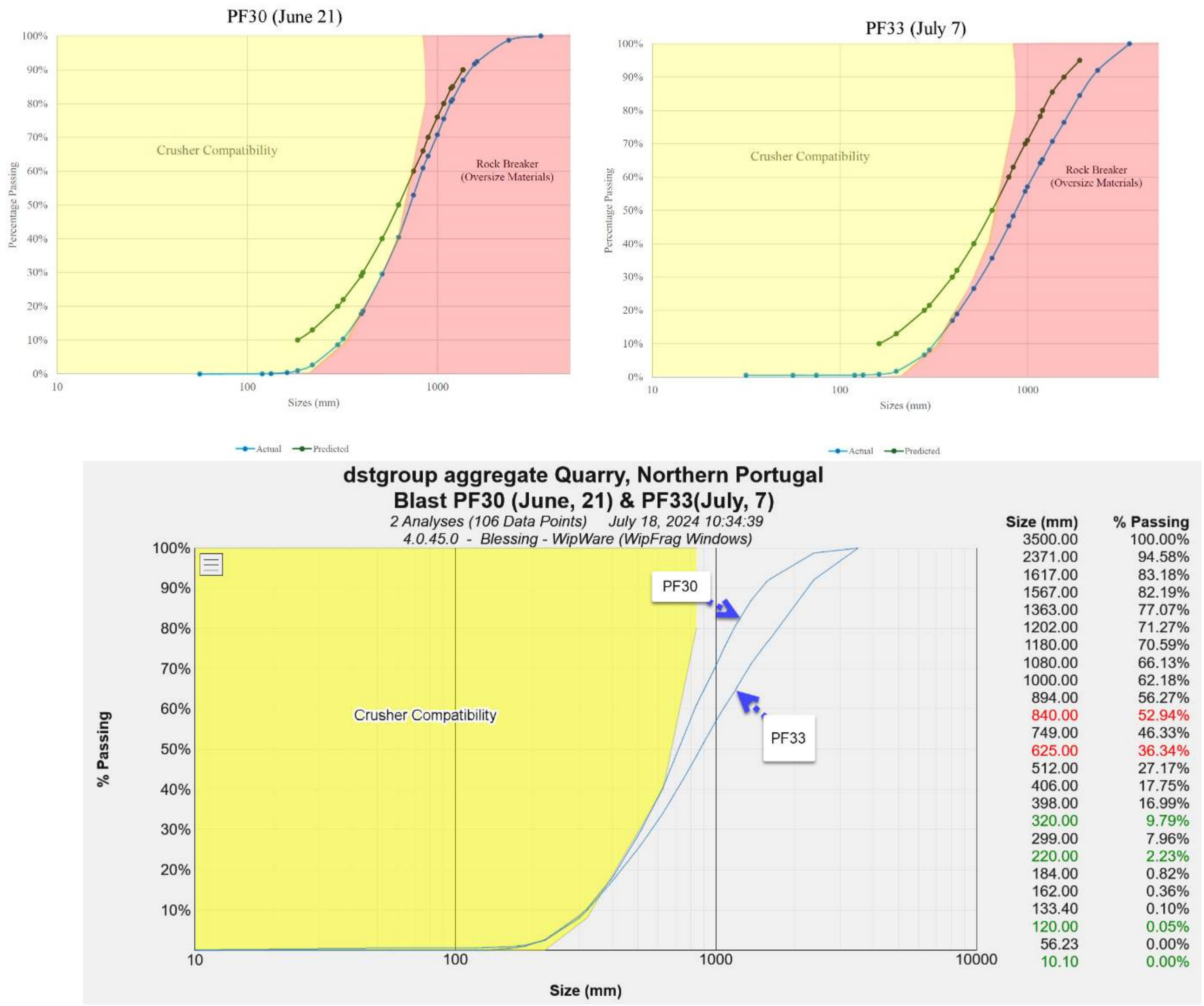

| Size (mm) | % Passing |
|---|---|
| 3500.00 | 100.00% |
| 2371.00 | 94.58% |
| 1617.00 | 83.18% |
| 1567.00 | 82.19% |
| 1363.00 | 77.07% |
| 1202.00 | 71.27% |
| 1180.00 | 70.59% |
| 1080.00 | 66.13% |
| 1000.00 | 62.18% |
| 894.00 | 56.27% |
| 840.00 | 52.94% |
| 749.00 | 46.33% |
| 625.00 | 36.34% |
| 512.00 | 27.17% |
| 406.00 | 17.75% |
| 398.00 | 16.99% |
| 320.00 | 9.79% |
| 299.00 | 7.96% |
| 220.00 | 2.23% |
| 184.00 | 0.82% |
| 162.00 | 0.36% |
| 133.40 | 0.10% |
| 120.00 | 0.05% |
| 56.23 | 0.00% |
| 10.10 | 0.00% |

**Figure 6. Crusher Compatibility Curve for PF 30 and PF 33 blasts.**

## Conclusion and Future Work

This study successfully developed and implemented a comprehensive mine-to-crusher framework tailored for aggregate quarry, establishing a baseline for assessing blasting results with a focus on crusher compatibility. The framework was applied to assess two blasts, revealing gaps between predicted and actual fragmentation outcomes. Key questions emerged from the assessment, such as identifying the reasons behind the discrepancies in fragmentation and determining which controllable parameters need adjustment to align the particle size distribution with the crusher compatibility zone. These insights will guide the next phase of this continuous improvement effort, targeting precise modifications to enhance overall operational efficiency and effectiveness. Future research will focus on addressing these questions and refining blast designs to achieve optimal crusher-compatible fragmentation. These changes aim to improve overall blast efficiency and ensure crusher compatibility.

## Acknowledgement

The authors appreciate dstgroup mining engineers, O-Pitblast and wipware Inc Technical team for their support during data collection and analysis for this paper.

## References

Bahloul, F., Hafsaoui, A., Idres, A., Boutarfa, F., Kanli, A. I., and Benselhoub, A. (2024). *Influence Of the Rock Mass Structure and The Blasting Technique on Blast Results in The Heliopolis Quarry.* Scientific Bulletin of National Mining University.

Dotto, M. S. ( 2024). Investigating the influence of discontinuity parameters on blast-induced fragmentation. *International Journal of Mining, Reclamation and Environment*, 1-25.

Ma, G. W., & An, X. M. . (2008). Numerical simulation of blasting-induced rock fractures. *International Journal of Rock Mechanics and Mining Sciences, 45*(6), 966-975.

Neale, A. M. (2010). Blast optimization at Kriel Colliery. *Journal of the Southern African Institute of Mining and Metallurgy, 110*(4), 161-168.

Nielsen, K., and Malvik, T. . (1999). Grindability enhancement by blast-induced microcracks. *Powder Technology, 105*(1-3), 52-56.

Rafeeian, N., Taji, M., & Nikkhah, A. . (2019). Mine to mill optimisation in Sarcheshmeh copper mine. *Helsinki Conference Proceedings, European Federation of Explosives Engineers.* Kerman, Iran. .

Roy, M. P., Paswan, R. K., Sarim, M. D., Kumar, S. U. R. A. J., Jha, R., & Singh, P. K. . (2016). Rock fragmentation by blasting-A review. *Journal of mines, metals and fuels, 64*(9), 424-431.

Saadatmand Hashemi, A., Katsabanis, P. . (2020). The Effect of Stress Wave Interaction and Delay Timing on Blast-Induced Rock Damage and Fragmentation. *Rock Mech Rock Eng, 53*, 2327–2346. doi: https://doi.org/10.1007/s00603-019-02043-9

Taji, M. (2014). *Structure of desired fragmentation by blast operation in metal mines.* Tehran: Research plan, Mining Industries Development and Renovation Organisation.

Workman, L., and Eloranta, J. (2003). The effects of blasting on crushing and grinding efficiency and energy consumption. *Proc 29th Con Explosives and Blasting Techniques, Int Society of Explosive Engineers* (pp. 1-5). Cleveland OH, : ISEE.